



Design, synthesis, and evaluation of novel racecadotril-tetrazole-amino acid derivatives as new potent analgesic agents

Mehdi Asadi¹, Maryam Mohammadi-Khanaposhtani², Faezeh Sadat Hosseini¹, Mahdi Gholami³, Ahmad Reza Dehpour^{4,5,*}, and Massoud Amanlou^{1,5,*}

¹Department of Medicinal Chemistry, Faculty of Pharmacy, Tehran University of Medical Sciences, Tehran, I.R. Iran.

²Cellular and Molecular Biology Research Center, Health Research Institute, Babol University of Medical Sciences, Babol, I.R. Iran.

³Department of Toxicology and Pharmacology, Faculty of Pharmacy and Toxicology and Poisoning Research Center, Tehran University of Medical Sciences, Tehran, I.R. Iran.

⁴Department of Pharmacology, School of Medicine, Tehran University of Medical Sciences, Tehran, I.R. Iran.

⁵Experimental Medicine Research Center, Tehran University of Medical Sciences, Tehran, I.R. Iran.

Abstract

Background and purpose: Although pain is one of the most common symptoms of diseases, it is often mismanaged due to limited access to painkillers and ineffectiveness, unacceptable side effects, or the possibility of abuse. However, an alternative approach to existing analgesics is to indirectly increase endogenous pain relief pathways by neprilysin (an enkephalinase) inhibitors. This enzyme breaks down and inactivates enkephalin, dynorphin, endorphins, and their derivatives.

Experimental approach: In this project, a new series of racecadotril-tetrazole-amino acid derivatives **15a-l** was synthesized and characterized on the basis of IR, ¹H and ¹³C NMR, mass spectrometry, and elemental analysis. The antinociceptive activity of synthesized compounds was assessed by a hot plate, tail-flick, and formalin assays in mice. Docking was used to identify the possible interactions between neprilysin and synthesized compounds.

Findings/Results: Most of the synthesized compounds showed moderate to good analgesic effects in hot plate and tail-flick test in comparison to morphine and racecadotril. Compounds **15i** and **15j** were the most potent compounds. The synergistic analgesic effect of compounds **15i** and **15j** with morphine and the antagonistic effect of naloxone on the activity of these compounds confirm that the analgesic effect of compounds **15i** and **15j** could be mediated through the opioidergic system. The negative and high binding energy of docking simulation of the most potent compounds in the catalytic site of neprilysin was also in good agreement with the inhibitory activity of test compounds.

Conclusion and implications: Racecadotril-tetrazole-amino acid derivatives, as potential antinociceptive agents, demonstrated moderate to good antinociceptive activities comparable with morphine and higher than racecadotril.

Keywords: Antinociceptive activity; Enkephalinase; Molecular docking simulation; Racecadotril; Tetrazole; Thiorphan.

INTRODUCTION

Palliative care is one of the most important fields of medical research. The most important reason for the importance of this field is that treating the cause of pain is not always possible. The most common medications used for the various types of pain are opioids and non-steroidal anti-inflammatory agents (1-5).

Opioids, in addition to abuse liability, are often associated with side effects such as constipation, vomiting, nausea, and respiratory depression (6).

*Corresponding author: M. Amanlou
Tel: +98-2166959067, Fax: +98-2164121111
Email: amanlou@tums.ac.ir

Access this article online



Website: <http://rps.mui.ac.ir>

DOI: 10.4103/1735-5362.319573

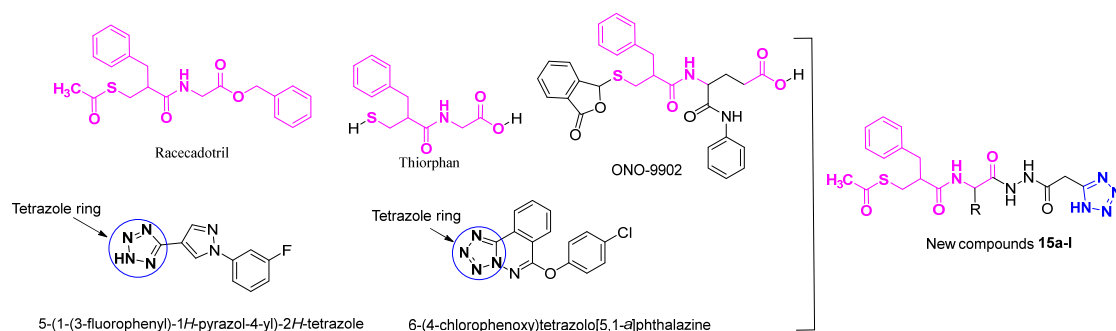


Fig. 1. Design strategy for racecadotril-tetrazole-amino acid derivatives **15a-l**.

Moreover, non-steroidal anti-inflammatory drugs created induced gastric and renal adverse effects, especially in those who need long-term pain management, such as malignancies and AIDS (7). Thus, the development of safe and effective pain relievers is an interesting subject for pharmaceutical chemists.

It is now well-documented that the endogenous opioid enkephalins are involved in the induction of analgesia and inhibition of their inactivating enzymes, enkephalinase, that led to potent physiological analgesic responses without significant side effects of morphine (the most widely-used opioid) and morphine-like agents (8-11).

Racecadotril (acetorphan) is the first orally available enkephalinase inhibitor that is used clinically as an antidiarrheal agent (Fig. 1) (12). This drug acts by increasing the local levels of enkephalin and stimulates opioid receptors (13). Furthermore, several studies demonstrated that thiorphan as an active metabolite of racecadotril has considerable antinociceptive activity (Fig. 1) (14). Furthermore, various thiorphan derivatives such as ONO-9902 have been reported as analgesic agents (15-17). As shown in Fig. 1, the latter compounds were obtained by modifications of the type of ester, the carboxylic acid group, and binding an amide group to the carbon attached to the amide group of thiorphan. One of the bioisosteres for the carboxylic acid group is the tetrazole ring (18).

On the other hand, several derivatives of tetrazole such as 5-(1-(3-fluorophenyl)-1H-pyrazol-4-yl)-2H-tetrazole and 6-(4-chlorophenoxy) tetrazolo [5,1-a]phthalazine with high analgesic effect have been reported (19,20). Therefore, using tetrazole and various

amino acids, we have designed and synthesized some new derivatives of racecadotril as potent analgesic compounds by hybridization approach strategy to produce new compounds with improved affinity and efficacy, compared to the parent drugs (Fig. 1, compounds **15a-l**) (21). These compounds were evaluated for their antinociceptive activities by a hot plate, tail-flick, and formalin assay. Furthermore, the synergic effect of these compounds with morphine and the effect of naloxone as an opioid antagonist on these compounds were evaluated. The mechanism of action of these compounds was evaluated by performing their docking study in the catalytic site of neprilysin (NEP), a zinc-dependent metalloprotease that cleaves small peptides such as enkephalins (22,23).

MATERIALS AND METHODS

Chemistry

All chemicals used in this study were obtained from Merck (Germany) and used without further purification. Morphine, racecadotril, and naloxone were purchased from Sigma-Aldrich Company (USA). Melting points were determined with a Kofler hot stage apparatus (Austria) and were uncorrected. Proton and carbon-13 nuclear magnetic resonance (^1H and ^{13}C NMR) spectra were recorded with a Bruker FT-500 (Germany), using tetramethylsilane as an internal standard. Coupling constant (J) values are presented in Hz, and spin multiples are given as s (singlet), d (doublet), t (triple), and m (multiple). Infrared (IR) spectra were acquired on a Nicolet Magna 550-FT spectrometer (USA). IR spectra of solid were recorded in KBr, and the absorption band was given in wavenumbers in cm^{-1} .

General procedure for the synthesis of 3-(acetylthio)-2-benzylpropanoic acid 5

A solution of benzyl malonic acid **1** (19.4 g, 100 mmol) in ethyl acetate was kept in an ice bath. Then, to the mentioned solution, formaldehyde **2** (5 g, 175 mmol) and Et₂NH (17.4 mL, 100 mmol) were added, and the obtained mixture was stirred at room temperature for 3 h. After finishing the benzyl malonic acid **1** (checked by thin-layer chromatography, TLC), the pH of the solution was set at 1 using HCl (1 N). After that, the ethyl acetate layer was separated by decanter, and the remaining residue was evaporated under reduced pressure, and the obtained 2-benzylacrylic acid **3** entered the next stage without purification. A mixture of 2-benzylacrylic acid **3** (12.6 g, 77 mmol) and thioacetic acid **4** (9 mL) in CH₂Cl₂ was heated at reflux for 3 h. After reaction completion, the excess thioacetic acid **4** was evaporated under reduced pressure, and the obtained oily residue was recrystallized from ethanol to give pure 3-(acetylthio)-2-benzylpropanoic acid **5** (24).

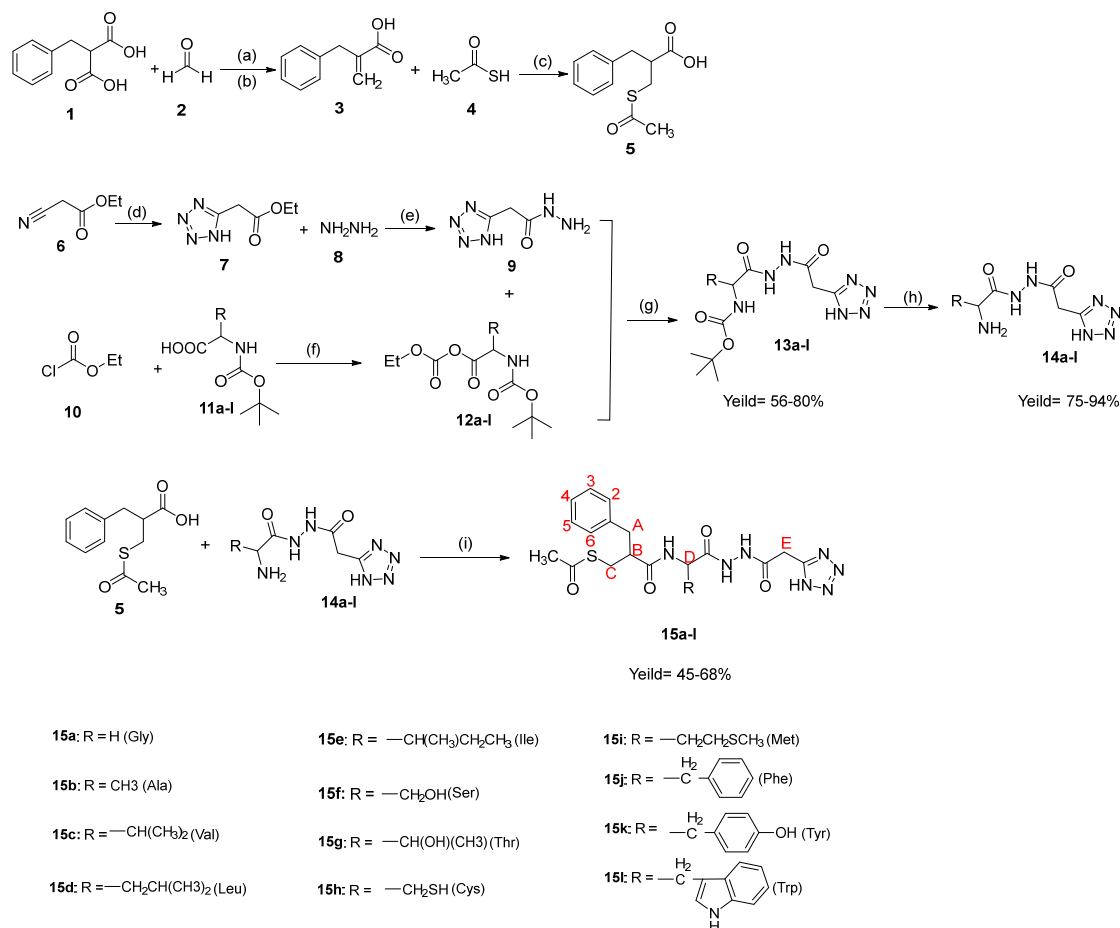
General procedure for the synthesis of tetrazole-amino acid derivatives 14a-l

A mixture of ethyl 2-cyanoacetate **6** (1 mmol), NaN₃ (0.5 mmol), and NH₄Cl (0.5 mmol) in dimethylformamide (DMF; 10 mL) was stirred at 80 °C for 8 h. After the ethyl cyanoacetate **6** was consumed (checked by TLC), water (20 mL) was added to the reaction mixture, and the pH of the mixture was set at 1 using HCl (1 N). At this moment, ethyl 2-(1*H*-tetrazol-5-yl)acetate **7** was formed as needle-shaped crystals, and after the filtration and recrystallization in ethyl acetate entered the next stage (25). In the next stage, a mixture of ethyl 2-(1*H*-tetrazol-5-yl)acetate **7** (1 mmol) and NH₂NH₂ (2 mmol) in ethanol was heated at reflux for 3 h. The reaction ran to completion when the color of the reaction mixture turned orange. Then, the reaction mixture was cooled down to room temperature to furnish a cream precipitate which was filtered off, washed with ethanol to obtain pure 2-(1*H*-tetrazol-5-yl)acetohydrazide **9** (25). On the other hand, ethyl chloroformate **10** (1 mmol) and Et₃N (1 mmol) in a dropwise manner were

added to a solution of protected amino acids **11a-l** (1 mmol) in dry tetrahydrofuran (THF; 10 mL) at -10 °C for 1 h to produce ethyl carbonic anhydride derivatives **12a-l**. Then, 2-(1*H*-tetrazol-5-yl)acetohydrazide **9** (1.1 mmol) was dissolved in H₂O (1 mL) and was added dropwise to the reaction mixture containing ethyl carbonic anhydride derivatives **12a-l**. At this moment, the reaction mixture's temperature was brought to ambient temperature and stirred for 5 h. After reaction completion, THF was evaporated under reduced pressure, H₂O (5 mL) was added to the residue, and the pH of residue was set at 1 using HCl (1 N). Then, the mixture was extracted using ethyl acetate and the organic phase was dried over Na₂SO₄, and the solvent was evaporated under reduced pressure to obtain pure compounds **13a-l**. To remove the protecting group from amino acid derivatives **13a-l**, trifluoroacetic acid (TFA; 10 mmol) was added to a solution of amino acid derivatives **13a-l** in H₂O and THF at 0 °C. The latter mixture was stirred at room temperature overnight. Then, a freeze-drying process was performed to produce the final products **14a-l**.

General procedure for the synthesis of racecadotril-tetrazol-amino acid derivatives 15a-l

N-(3-Dimethylaminopropyl)-N'-ethylcarbodiimide HCl/hydroxybenzotriazole (EDC/HOBT; 1.1 mmol) and Et₃N (1 mmol) were added to a solution of 3-(acetylthio)-2-benzylpropanoic acid **5** (1 mmol) in DMF at 0 °C and the obtained mixture was brought to room temperature. At this moment, tetrazole-amino acid derivatives **14a-l** were added to the reaction mixture and the final mixture was stirred at room temperature for 16 h. After completing the reaction (checked by TLC), the reaction mixture was extracted first with citric acid and then with a saturated bicarbonate solution. Finally, the obtained organic phase was washed with water and brine. This organic phase was dried over Na₂SO₄, and the solvent was evaporated under reduced pressure to obtain pure target compounds **15a-l**. The synthetic procedure for new racecadotril-tetrazole-amino acid derivatives **15a-l** is shown in Scheme 1.



Scheme 1. Reagents and conditions for the synthesis of compounds **15a-l**: (a) EtOAc, Et₂NH, 0 °C, 3 h; (b) pH adjust to 1 (HCl 1N); (c) CH₂Cl₂, reflux, 3 h, yield = 58%; (d) NH₄Cl, NaN₃, DMF, 80 °C, 8 h, yield = 80%; (e) EtOH, reflux, 3 h; (f) Et₃N, tetrahydrofuran, -10 °C, 1 h; (g) H₂O, tetrahydrofuran, RT, 3 h; (h) trifluoroacetic acid, tetrahydrofuran, H₂O, RT, overnight; (i) EDC/HOBT, DMF, Et₃N, RT, 16 h.

Antinociceptive activity tests

Animals and drugs

Male mice (Pasteur Institute of Iran, Tehran, Iran), weighing 20-25 g, were used as experimental animals. Mice were housed in 25-30 °C, 12/12-h light/dark cycle, and allowed to acclimatize with free access to water and food for a 24 h period before testing. Animals were randomly arranged into experimental groups, and each mouse was applied only once for the experiments. Morphine, as an opioid agonist, racecadotril, as an enkephalinase inhibitor, and naloxone as a standard opioid antagonist were also used in this study. The protocols for the study were approved by Pharmaceutical Sciences Research Center Ethics Committee (Ethics No. IR.TUMS.PSRC.REC.1396.3503).

Hot plate test

The antinociceptive activity of the novel compounds was determined with a hot-plate test (26,27). In this model of induced pain, a compound's ability to produce anti-pain effects in mice was based on the observation of the reaction to pain caused by heat. In the conventional hot plate method, the hot plate temperature was maintained at 52°C, and the unrestrained animals were allowed to place on the plate until a nocifensive behavior is observed. The newly synthesized compounds **15a-l**, morphine and racecadotril were dissolved in 5% DMSO (in saline) and injected intraperitoneally (i.p.) 60 min before the stress exposure in the doses of 20, 40, and 80 mg/kg for the new compounds and racecadotril and

5 mg/kg for morphine, respectively. As inescapable stress (a 2-mA electric foot-shock) was delivered in 60×16 msec pulses once every 2 s for 3 min to mice. After 60 min of the stress exposure, jump latencies on a 52 °C were measured.

Tail-flick test

The antinociceptive activity of the newly synthesized compounds **15a-1** was also evaluated using the tail-flick test method (28). In this assay, the latency time for the tail withdrawal reflex was measured. Mice were gently held with the tail put on the tail-flick apparatus (Ugo Basile, Italy), and the tail-flick response was elicited by using a radiant heat stimulus to the ventral surface of the rat-tail about 3-4 cm from the tip of the tail. The time in seconds, from initial heat source activation until tail withdrawal, was recorded.

Formalin test

In the formalin test, mice were injected (i.p) with saline, morphine (5 mg/kg), newly synthesized compounds (20, 40, and 80 mg/kg) and racecadotril (20, 40, and 80 mg/kg) and 30 min later received 2 μ L of the 1% formalin solution into the plantar surface of the right paw (29). Briefly, in two phases, the number of paw licking was measured: phase 1, 5 min after formalin injection, and phase 2, 20 min after formalin injection.

Docking study

Molecular docking was used to identify the possible interactions between NEP (enkephalinase) and synthesized compounds. AutoDockTools 1.5.6 (ADT) (30,31) was used to prepare all receptor and ligands' input files and analyze the result. The NEP crystal structure as receptor was retrieved from a protein data bank with PDB ID: 1R1H (29). Redocking of co-crystal ligand was used to validate the docking method with obtained root mean square deviation (RMSD) lower than 2. All water molecules and ions were removed from the crystal structure to prepare the receptor file then polar hydrogen was added, and non-polar hydrogen was merged. The Kollman-united charges were added and the receptor file saved in pdbqt format. The 2D-

structures of the ligands were sketched by MarvinSketch version 15.2.2, converted to 3D-structures and optimized, and saved in PDB format by Chem3D ultra version 8.0. Rotatable bonds and Gasteiger-Marsili charges were added to all ligands and then saved in pdbqt format. A $50 \times 50 \times 50$ Å (x, y, and z) grid box was centered on the NEP's active site with 0.375 Å grid point spacing in each dimension (31). AutoGrid4.2 was used to prepare grid maps of each atom type. Docking parameters were set as a Lamarckian genetic algorithm with run job = 30, initial population = 150, and the maximum energy evaluation = 2.5×10^5 and the default value for other parameters (32). Autodock4 Zn carried out molecular docking (33). Docking procedures were applied automatically by scripts written in-house. Visualization of the most favorable docking poses has been done by PyMol version 1.1eval and LIGPLOT version v.2.2 (34,35).

Statistical analysis

Statistical analysis was made with the GraphPad Prism (Ver.8.4, USA). The results are presented as the mean \pm SEM in each experimental group. The data were analyzed by one-way analysis of variance (ANOVA) followed by Dunnett post-hoc test for multiple comparisons between groups. In all experiments, $P < 0.05$ considered as significant.

RESULTS

Chemistry

Chemical structures of all synthesized derivatives were confirmed by IR, mass spectrometry (MS), ¹H NMR and ¹³C NMR methods. The results of spectral analysis of products are presented below:

S-(3-((2-(2-(2-(1H-tetrazol-5-yl)acetyl)hydrazineyl)-2-oxoethyl)amino)-2-benzyl-3-oxopropyl)ethanethioate (15a)

White solid; yield: 74% (310.1 mg); mp: 128-130 °C; IR (KBr): 3476 (NH), 3419 (NH), 3129 (C-H aromatic), 1708 (C=O), 1618 (C=N) cm^{-1} ; ¹H NMR (D₂O, 500 MHz) δ (ppm): 10.12 (s, 2H, NH-hydrazide), 8.29 (t, $J = 8.7$ Hz, 1H, NH-amid), 7.37-7.33 (m, 3H, H-2, H-4, H-6), 7.24 (t, $J = 8.4$ Hz, 2H, H-3, H-5), 3.99 (s, 1H,

CH-B), 3.69 (d, $J = 15$ Hz, 1H, CH-E), 3.63 (d, $J = 15$ Hz, 1H, CH-E'), 3.55-3.27 (m, 2H, CH₂-D), 3.35 (m, 2H, CH₂-A), 3.05-2.72 (m, 2H, CH₂-C), 1.93 (s, 3H, CH₃) ppm; ¹³C NMR (D₂O, 125 MHz) δ (ppm): 182.2, 170.3, 166.6, 166.2, 159.7, 137.9, 132.8, 129.0, 128.7, 126.9, 123.7, 48.8, 42.7, 37.9, 33.3, 30.9, 29.9 ppm; EI-MS: m/z (%) 419 (M+, 30), 376 (82), 328 (43), 279 (81), 244 (35), 216 (51), 141 (100), 119 (75), 55 (38); Anal. Calcd. for C₁₇H₂₁N₇O₄S: C, 48.68; H, 5.05; N, 23.38. Found: C, 48.31; H, 5.19; N, 23.02.

S-(3-(1-(2-(2-(1H-tetrazol-5-yl) acetyl) hydrazineyl)-1-oxopropan-2-yl) amino)-2-benzyl-3-oxopropyl)ethanethioate (15b)

White solid; yield: 81% (373.4 mg); mp: 134-136 °C; IR (KBr): 3413 (NH), 3071 (C-H aromatic), 1706 (C=O), 1618 (C=N) cm⁻¹; ¹H NMR (D₂O, 500 MHz) δ (ppm): 9.81 (s, 2H, NH-hydrazide), 8.09 (d, $J = 7.0$ Hz, 1H, NH-amid), 7.34 (d, $J = 8.1$ Hz, 2H, H-2, H-6), 7.27 (t, $J = 8.1$ Hz, 2H, H-3, H-5), 7.21 (t, $J = 8.1$ Hz, 1H, H-4), 3.87-3.84 (m, 1H, CH-B), 3.64 (d, $J = 15$ Hz, 1H, CH-E), 3.40 (m, 1H, CH-D), 3.27 (d, $J = 15$ Hz, 1H, CH-E), 3.15-3.13 (m, 2H, CH₂-A), 3.08-3.03 (m, 2H, CH₂-C), 2.03 (s, 3H, CH₃), 2.03 (d, $J = 7.0$ Hz, 3H, CH₃) ppm; ¹³C NMR (D₂O, 125 MHz) δ (ppm): 183.4, 170.0, 165.0, 164.5, 157.6, 133.5, 131.0, 124.0, 123.3, 48.1, 47.5, 37.7, 33.3, 30.9, 29.8, 18.1 ppm; EI-MS: m/z (%) 433 (M+, 73), 390 (59), 323 (43), 293 (59), 222 (62), 212 (100), 141 (83), 105 (83), 55 (48); Anal. Calcd. for C₁₈H₂₃N₇O₄S: C, 49.87; H, 5.35; N, 22.62. Found: C, 49.51; H, 5.73; N, 22.35.

S-(3-(1-(2-(2-(1H-tetrazol-5-yl) acetyl) hydrazineyl)-3-methyl-1-oxobutan-2-yl) amino)-2-benzyl-3-oxopropyl)ethanethioate (15c)

White solid; yield: 79% (318.4 mg); mp: 139-141 °C; IR (KBr): 3476 (NH), 3415 (NH), 3129 (C-H aromatic), 1707 (C=O), 1618 (C=N) cm⁻¹; ¹H NMR (D₂O, 500 MHz) δ (ppm): 10.08 (s, 2H, NH-hydrazide), 8.07 (d, $J = 8.5$ Hz, 1H, NH-amid), 7.38 (d, $J = 8.2$ Hz, 2H, H-2, H-6), 7.27 (t, $J = 8.2$ Hz, 2H, H-3, H-5), 7.19 (t, $J = 7.5$ Hz, 1H, H-4), 3.86-3.84 (m, 1H, CH-B), 3.60 (d, $J = 13.5$ Hz, 1H, CH-E), 3.44-3.40 (m, 2H, CH-E', CH-D), 3.29-3.21 (m, 3H, CH₂-A,

CH-C), 3.17-3.13 (m, 1H, CH-C'), 2.55-2.51 (m, 1H, CH-F), 2.04 (s, 3H, CH₃), 1.07 (d, $J = 6.5$ Hz, 6H, 2×CH₃) ppm; ¹³C NMR (D₂O, 125 MHz) δ (ppm): 183.1, 170.6, 165.3, 164.9, 156.7, 137.5, 132.9, 126.1, 124.5, 123.9, 62.5, 59.3, 48.1, 37.1, 31.5, 28.5, 28.0, 19.7 ppm; EI-MS: m/z (%) 461 (M+, 42), 418 (39), 321 (59), 141 (100), 55 (35); Anal. Calcd. for C₂₀H₂₇N₇O₄S: C, 52.05; H, 5.90; N, 21.24. Found: C, 51.78; H, 5.63; N, 20.98.

S-(3-(1-(2-(2-(1H-tetrazol-5-yl) acetyl) hydrazineyl)-4-methyl-1-oxopentan-2-yl) amino)-2-benzyl-3-oxopropyl)ethanethioate (15d)

White solid; yield: 72% (342.4 mg); mp: 142-144 °C; IR (KBr): 3456 (NH), 3085 (C-H aromatic), 1712 (C=O), 1625 (C=N) cm⁻¹; ¹H NMR (D₂O, 500 MHz) δ (ppm): 10.25 (s, 2H, NH-hydrazide), 8.12 (d, $J = 6.5$ Hz, 1H, NH-amid), 7.37-7.33 (m, 3H, H-2, H-4, H-6), 7.25 (t, $J = 8.4$ Hz, 2H, H-3, H-5), 3.96 (m, 1H, CH-B), 3.63-3.57 (m, 2H, CH₂-E), 3.01-2.96 (m, 3H, CH₂-A, CH-D), 2.87-2.64 (m, 2H, CH₂-C), 1.99 (s, 3H, CH₃), 1.47-1.43 (m, 1H, CH-F), 1.19-1.16 (m, 1H, CH-F'), 0.82 (dd, $J = 15.5$, 6.5 Hz, 6H, 2×CH₃) ppm; ¹³C NMR (D₂O, 125 MHz) δ (ppm): 182.2, 172.4, 169.6, 162.5, 157.7, 129.4, 128.2, 126.0, 125.6, 56.1, 54.6, 45.7, 36.9, 28.3, 25.4, 24.9, 24.1, 18.9 ppm; EI-MS: m/z (%) 475 (M+, 61), 432 (27), 369 (94), 254 (45), 222 (84), 106 (69), 55 (24); Anal. Calcd. for C₂₁H₂₉N₇O₄S: C, 53.04; H, 6.15; N, 20.62. Found: C, 53.35; H, 6.40; N, 20.78.

S-(3-(1-(2-(2-(1H-tetrazol-5-yl) acetyl) hydrazineyl)-3-methyl-1-oxopentan-2-yl) amino)-2-benzyl-3-oxopropyl)ethanethioate (15e)

White solid; yield: 53% (251.7 mg); mp: 145-147 °C; IR (KBr): 3423 (NH), 2995 (C-H aromatic), 1716 (C=O), 1618 (C=N) cm⁻¹; ¹H NMR (D₂O, 500 MHz) δ (ppm): 10.41 (s, 2H, NH-Hydrazide), 8.24 (d, $J = 7.35$ Hz, 1H, NH-amid), 7.45 (t, $J = 8.1$ Hz, 2H, H-3, H-5), 7.37 (dd, $J = 8.1$, 3.5 Hz, 2H, H-2, H-6), 7.26 (t, $J = 7.5$ Hz, 1H, H-4), 3.62 (m, 1H, CH-B), 3.14 (d, $J = 14.5$ Hz, 1H, CH-E), 2.90 (d, $J = 14.5$ Hz, 1H, CH-E'), 2.74 (d, $J = 8.3$ Hz, 1H, CH-D), 2.51-2.45 (m, 2H, CH-A), 2.27 (d, $J = 14.5$ Hz, 1H, CH-C), 2.2 (d, $J = 14.5$ Hz, 1H, CH-C'),

1.99 (s, 3H, CH₃), 1.62 (m, 2H, CH-G), 1.40-1.37 (m, 1H, CH-F), 0.83 (d, $J = 6.8$ Hz, 3H, CH₃), 0.71 (t, $J = 6.8$ Hz, 3H, CH₃) ppm; ¹³C NMR (D₂O, 125 MHz) δ (ppm): 182.1, 171.9, 169.2, 166.0, 157.4, 139.2, 129.9, 128.6, 128.3, 128.1, 125.3, 57.3, 46.4, 38.4, 31.7, 29.7, 25.5, 25.1, 20.6, 17.7 ppm; EI-MS: m/z (%) 475 (M⁺, 64), 364 (100), 335 (68), 289 (87), 254 (43), 222 (63), 150 (09), 55 (09); Anal. Calcd. for C₂₁H₂₉N₇O₄S: C, 53.04; H, 6.15; N, 20.62. Found: C, 53.51; H, 6.48; N, 20.24.

S-(3-(1-(2-(2-(1H-tetrazol-5-yl) acetyl) hydrazineyl)-4-(methylthio)-1-oxobutan-2-yl) amino)-2-benzyl-3-oxopropyl) ethanethioate (15f)

White solid; yield: 66% (325.4 mg); mp: 153-155 °C; IR (KBr): 3412 (NH), 3020 (C-H aromatic), 1717 (C=O), 1618 (C=N) cm⁻¹; ¹H NMR (D₂O, 500 MHz) δ (ppm): 10.10 (s, 2H, NH-hydrazide), 8.03 (d, $J = 7.7$ Hz, 1H, NH-amid), 7.36-7.28 (m, 3H, H-3, H-4, H-5), 7.07 (d, $J = 8.5$ Hz, 2H, H-2, H-6), 3.58-3.55 (m, 1H, CH-B), 3.48-3.43 (m, 2H, CH₂-E), 3.20-3.17 (dd, $J = 10.5, 5.5$ Hz, 2H, CH-D), 2.87-2.64 (m, 2H, CH₂-C), 2.69-2.59 (m, 2H, CH₂-G), 2.34 (s, 3H, CH₃) 2.09-1.98 (m, 2H, CH-F), 1.90 (s, 3H, CH₃) ppm; ¹³C NMR (D₂O, 125 MHz) δ (ppm): 183.5, 170.6, 167.3, 164.9, 158.0, 138.4, 130.0, 129.2, 129.1, 127.6, 127.5, 56.6, 45.1, 41.1, 34.4, 29.5, 28.1, 15.4 ppm; EI-MS: m/z (%) 493 (M⁺, 22), 382 (12), 353 (37), 222 (14), 141 (56), 127 (100), 55 (20); Anal. Calcd. for C₂₀H₂₇N₇O₄S₂: C, 48.67; H, 5.51; N, 19.86. Found: C, 48.94; H, 5.87; N, 20.12.

S-(3-(1-(2-(2-(1H-tetrazol-5-yl) acetyl) hydrazineyl)-3-hydroxy-1-oxopropan-2-yl) amino)-2-benzyl-3-oxopropyl) ethanethioate (15g)

White solid; yield: 62% (278.4 mg); mp: 128-130 °C; IR (KBr): 3467 (NH), 3416 (NH), 3158 (C-H aromatic), 1722 (C=O), 1691 (C=O), 1618 (C=N) cm⁻¹; ¹H NMR (D₂O, 500 MHz) δ (ppm): 10.00 (s, 2H, NH-Hydrazide), 8.08 (d, $J = 6.5$ Hz, 1H, NH-amid), 7.24 (dd, $J = 7.1, 2.5$ Hz, 2H, H-2, H-6), 7.20-7.13 (m, 3H, H-3, H-4, H-5), 3.82 (m, 2H, CH₂-F), 3.51-3.49 (m, 1H, CH-B), 3.37 (t, $J = 6.9$ Hz, 1H, CH-D), 3.11 (d, $J = 13.9$ Hz, 1H, CH-E), 2.87 (d, $J = 13.9$ Hz, 1H, CH-E'), 2.73-2.68 (m, 2H, CH₂-

A), 2.53 (d, $J = 13.0$ Hz, 1H, CH-C), 2.39 (d, $J = 13.5$ Hz, 1H, CH-C'), 1.82 (s, 3H, CH₃) ppm; ¹³C NMR (D₂O, 125 MHz) δ (ppm): 184.6, 171.2, 165.3, 164.0, 159.9, 138.4, 129.5, 128.6, 126.7, 47.8, 47.5, 40.9, 37.4, 28.2 ppm; EI-MS: m/z (%) 449 (M⁺, 39), 329 (11), 309 (33), 228 (65), 222 (40), 155 (100), 141 (79), 104 (20), 55 (17); Anal. Calcd. for C₁₈H₂₃N₇O₅S: C, 48.10; H, 5.16; N, 21.81. Found: C, 48.36; H, 5.29; N, 21.67.

S-(3-(1-(2-(2-(1H-tetrazol-5-yl) acetyl) hydrazineyl)-3-hydroxy-1-oxobutan-2-yl) amino)-2-benzyl-3-oxopropyl) ethanethioate (15h)

White solid; yield: 55% (254.6 mg); mp: 131-133 °C; IR (KBr): 3471 (NH), 3416 (NH), 3117 (C-H aromatic), 1720 (C=O), 1618 (C=N) cm⁻¹; ¹H NMR (D₂O, 500 MHz) δ (ppm): 10.07 (s, 2H, NH-hydrazide), 8.12 (d, $J = 7.8$ Hz, 1H, NH-amid), 7.20 (t, $J = 7.7$ Hz, 2H, H-3, H-5), 7.16 (d, $J = 7.3$ Hz, 2H, H-2, H-6), 7.11 (t, $J = 7.8$ Hz, 1H, H-4), 3.83 (m, 1H, CH-F), 3.59 (m, 1H, CH-B), 3.35 (t, $J = 7.5$ Hz, 1H, CH-D), 3.07 (d, $J = 14.5$ Hz, 1H, CH-E), 2.95 (d, $J = 14.5$ Hz, 1H, CH-E'), 2.73-2.65 (m, 2H, CH₂-A), 2.63-2.49 (m, 2H, CH₂-C), 2.06 (s, 3H, CH₃), 0.76 (t, $J = 7.9$ Hz, 3H, CH₃), 1.19-1.15 (m, 1H, CH-F'), 0.82 (dd, $J = 15.5, 6.5$ Hz, 6H, 2×CH₃) ppm; ¹³C NMR (D₂O, 125 MHz) δ (ppm): 184.6, 171.3, 163.3, 161.4, 157.1, 139.7, 129.0, 128.9, 128.5, 125.9, 125.8, 57.7, 46.3, 38.6, 31.4, 30.9, 28.3, 15.6 ppm; EI-MS: m/z (%) 463 (M⁺, 85), 352 (100), 322 (86), 246 (76), 222 (42), 141 (28), 55 (28); Anal. Calcd. for C₁₉H₂₅N₇O₅S: C, 49.23; H, 5.44; N, 21. Found: C, 49.54; H, 5.80; N, 59.

S-(3-(1-(2-(2-(1H-tetrazol-5-yl) acetyl) hydrazineyl)-3-mercapto-1-oxopropan-2-yl) amino)-2-benzyl-3-oxopropyl)ethanethioate (15i)

White solid; yield: 76% (353.4 mg); mp: 142-144 °C; IR (KBr): 3456 (NH), 3085 (C-H aromatic), 1712 (C=O), 1625 (C=N) cm⁻¹; ¹H NMR (D₂O, 500 MHz) δ (ppm): 10.07 (s, 2H, NH-hydrazide), 8.24 (d, $J = 8.5$ Hz, 1H, NH-amid), 7.27 (d, $J = 7.5$ Hz, 2H, H-2, H-6), 7.22-7.17 (m, 3H, H-3, H-4, H-5), 3.85-3.80 (m, 1H, CH-B), 3.63 (d, $J = 12.1$ Hz, 1H, CH-E), 3.62-3.35 (m, 2H, CH-E', CH-D), 3.15-3.11 (m,

2H, CH₂-A), 2.86-2.81 (m, 1H, CH-F), 2.79-2.75 (m, 1H, CH-F'), 2.055 (s, 3H, CH₃), 1.89 (t, *J* = 12.1 Hz, 1H, SH) ppm; ¹³C NMR (D₂O, 125 MHz) δ (ppm): 183.6, 170.2, 165.4, 163.0, 158.4, 136.6, 127.7, 124.5, 124.0, 54.3, 49.2, 47.8, 38.3, 35.5, 31.1, 29.3, 28.8 ppm; EI-MS: *m/z* (%) 455 (M⁺, 18), 354 (14), 324 (39), 244 (33), 222 (74), 141 (100), 55 (20); Anal. Calcd. for C₁₇H₂₃N₇O₄S₂: C, 46.44; H, 4.98; N, 21.06. Found: C, 46.72; H, 5.18; N, 21.35.

***S*-(3-(1-(2-(2-(1*H*-tetrazol-5-yl) acetyl) hydrazineyl)-1-oxo-3-phenylpropan-2-yl) amino)-2-benzyl-3-oxopropyl) ethanethioate (15j)**

White solid; yield: 85% (432.6 mg); mp: 163-165 °C; IR (KBr): 3479 (NH), 3416 (NH), 3023 (C-H aromatic), 1723 (C=O), 1627 (C=N) cm⁻¹; ¹H NMR (D₂O, 500 MHz) δ (ppm): 10.1 (s, 2H, NH-hydrazide), 8.14 (d, *J* = 7.9 Hz, 1H, NH-amid), 7.41 (t, *J* = 8.2 Hz, 1H, H-4), 7.29-7.26 (m, 4H, H-3, H-5, H-3', H-5'), 7.21-7.19 (m, 2H, H-2', H-6'), 7.15-7.11 (m, 2H, H-2, H-6), 7.08 (t, *J* = 7.85 Hz, 1H, H-4'), 3.50 (m, 1H, CH-B), 3.17-3.12 (m, 2H, CH₂-E), 2.93-2.86 (m, 3H, CH₂-A, CH-D), 2.80 (d, *J* = 12.0 Hz, 1H, CH-F), 2.68-2.63 (m, 1H, CH-F'), 2.52 (d, *J* = 8.0 Hz, 2H, CH₂-C), 1.93 (s, 3H, CH₃) ppm; ¹³C NMR (D₂O, 125 MHz) δ (ppm): 184.6, 171.9, 166.1, 164.0, 158.2, 136.2, 128.5, 128.3, 124.1, 118.7, 56.5, 45.3, 37.4, 30.5, 28.3, 27.0 ppm; EI-MS: *m/z* (%) 509 (M⁺, 25), 369 (56), 288 (37), 222 (60), 195 (100), 141 (75), 55 (49); Anal. Calcd. for C₂₄H₂₇N₇O₄S: C, 56.57; H, 5.34; N, 19.24. Found: C, 56.82; H, 5.59; N, 19.41.

***S*-(3-(1-(2-(2-(1*H*-tetrazol-5-yl) acetyl) hydrazineyl) -3-(4-hydroxyphenyl) -1-oxopropan-2-yl) amino)-2-benzyl-3-oxopropyl) ethanethioate (15k)**

White solid; yield: 74% (314.5 mg); mp: 150-152 °C; IR (KBr): 3473 (NH), 3387 (NH), 3087 (C-H aromatic), 1717 (C=O), 1622 (C=N) cm⁻¹; ¹H NMR (D₂O, 500 MHz) δ (ppm): 10.03 (s, 2H, NH-hydrazide), 8.15 (d, *J* = 7.3 Hz, 1H, NH-amid), 7.53 (d, *J* = 8.5 Hz, 2H, H-2', H-6'), 7.42 (d, *J* = 6.9 Hz, 2H, H-2, H-6), 7.36 (t, *J* = 7.0 Hz, 2H, H-3, H-5), 7.28 (t, *J* = 6.9 Hz, 1H, H-4), 6.92 (d, *J* = 8.5 Hz, 2H, H-3', H-5'), 3.78-3.74 (m, 1H, CH-B), 3.62 (d, *J* = 14.8

Hz, 1H, H-E), 3.42 (d, *J* = 14.8 Hz, 1H, H-E'), 3.28-3.24 (m, 3H, CH₂-A, CH-D), 3.15-3.11 (m, 2H, CH₂-F), 2.55-2.51 (m, 2H, CH₂-C), 2.00 (s, 3H, CH₃), ppm; ¹³C NMR (D₂O, 125 MHz) δ (ppm): 180.5, 177.1, 170.0, 165.8, 164.0, 157.0, 138.1, 130.1, 129.3, 127.6, 127.4, 124.1, 119.4, 54.3, 47.7, 41.7, 34.8, 30.1, 27.7 ppm; EI-MS: *m/z* (%) 525 (M⁺, 54), 385 (76), 328 (59), 222 (23), 160 (75), 144 (100), 54 (25); Anal. Calcd. for C₂₄H₂₇N₇O₅S: C, 54.85; H, 5.18; N, 18.66. Found: C, 54.48; H, 4.87; N, 18.32.

***S*-(3-(1-(2-(2-(1*H*-tetrazol-5-yl) acetyl) hydrazineyl)-3-(1*H*-indol-3-yl)-1-oxopropan-2-yl) amino)-2-benzyl-3-oxopropyl) ethanethioate (15l)**

White solid; yield: 64% (350.7); mp: 167-169 °C; IR (KBr): 3479 (NH), 3414 (NH), 3095 (C-H aromatic), 1707 (C=O), 1620 (C=N) cm⁻¹; ¹H NMR (D₂O, 500 MHz) δ (ppm): 9.83-9.94 (s, 2H, NH-hydrazide), 8.22 (d, *J* = 7.9 Hz, 1H, NH-amid), 8.91 (d, *J* = 7.7 Hz, 1H, H-4'), 7.79 (s, 1H, H-2'), 7.60-7.57 (m, 2H, H-5', H-6'), 7.32 (d, *J* = 7.8 Hz, 2H, H-2, H-6), 7.26-7.23 (m, 3H, H-3, H-4, H-5), 7.11 (d, *J* = 7.7 Hz, 1H, H-7'), 3.86-3.81 (m, 1H, CH-B), 3.63 (d, *J* = 13.3 Hz, 1H, CH-E), 3.42 (d, *J* = 13.3 Hz, 1H, CH-E'), 3.29-3.24 (m, 3H, CH₂-A, CH-D), 3.16-3.13 (m, 2H, CH₂-F), 2.69-3.65 (m, 2H, CH₂-C), 2.05 (s, 3H, CH₃) ppm; ¹³C NMR (D₂O, 125 MHz) δ (ppm): 182.1, 170.3, 166.3, 164.1, 158.5, 137.5, 131.8, 130.8, 129.9, 129.6, 127.4, 127.1, 119.7, 119.2, 117.3, 116.8, 56.6, 49.2, 42.0, 37.3, 30.1, 28.0, 27.7 ppm; EI-MS: *m/z* (%) 548 (M⁺, 59), 505 (80), 408 (25), 327 (52), 222 (100), 141 (86), 99 (44), 55 (27); Anal. Calcd. for C₂₆H₂₈N₈O₄S: C, 56.92; H, 5.14; N, 20.42. Found: C, 56.71; H, 5.29; N, 20.77.

Antinociceptive activity

The antinociceptive activity of the racecadotril-tetrazole-amino acid derivatives **15a-1** was evaluated by hot-plate, tail-flick, and formalin tests (26-28). Antinociceptive activity of these compounds was compared to morphine as a standard opioid agonist and racecadotril as an enkephalinase inhibitor. Moreover, to achieve a potent antinociceptive agent, various amino acids were used in the synthesis of the

title compounds **15a-l** (Scheme 1). Enzymes of the peptidase family, such as enkephalinases, especially NEP, have two additional hydrophobic binding pockets, anionic binding sites, and Zn ion as a cofactor in their active site. Based on this finding, enzyme inhibitors such as lisinopril and enalaprilat have already been designed and synthesized (36). In this study, different amino acids were used to investigate the effect of side-chain on binding to hydrophobic pockets at the active site of the enzyme to increase binding properties and inhibitory activity.

Hot plate test

The first analgesic evaluation in this study was the hot-plate test. In the latter assay, the latency time value for morphine as a standard analgesic drug at 5 mg/kg at time zero was 4.21 ± 0.38 s, and 60 min after injection was 11.72 ± 0.21 s. As shown in Table 1, the comparison of latency time values of the new compounds **15a-l** at 20 mg/kg with morphine at 5 mg/kg revealed that all the synthesized compounds, except for isoleucine derivative **15e** and glycine derivative **15a**, were more analgesic than morphine.

The combined targets and their mechanisms were investigated by the effects of synergism and their antagonism on concomitant use with morphine and naloxone. For this purpose, the synergic effect of the most potent compounds (compounds **15i** and **15j**) with morphine and the antagonist effect of naloxone on these new

compounds were also evaluated in the hot plate assay (Fig. 2). As shown in Fig. 2, racecadotril's synergic effect with the morphine and antagonist effect of naloxone on racecadotril is not significant, while the latter effects on the compounds **15i** and **15j** are considerable.

Tail-flick test

The second antinociceptive evaluation in this study was tail-flick assay. In this assay, the latency time value for morphine at 5 mg/kg at 0 min was 3.38 ± 0.26 s, and 60 min after injection was 10.6 ± 0.281 s (Table 2).

The synergic effect of the most potent compounds **15i**, **15j**, and racecadotril with morphine was evaluated by a tail-flick test. As shown in Fig. 3, these assays demonstrated that the newly synthesized compounds created a synergic effect with morphine, while racecadotril with morphine did not create a synergic effect. The antagonist effect of naloxone on new compounds **15i**, **15j**, and parent compound, racecadotril, was also evaluated by tail-flick test. According to the obtained data, analgesic effects of racecadotril and compounds **15i** and **15j** were antagonized by naloxone (Fig. 3).

Formalin test

The third assay to evaluate the analgesic effects of the newly synthesized compounds **15a-l** was the formalin test. The obtained result was listed in Table 3.

Table 1. Analgesic effect of the synthesized compounds 15a-l in comparison to morphine and racecadotril using hot plate method.

Compound	Latency time (s) (20 mg/kg)		Latency time (s) (40 mg/kg)		Latency time (s) (80 mg/kg)		ED ₅₀ (mg/kg)
	0 min	60 min	0 min	60 min	0 min	60 min	
15a	4.14 ± 0.68	11.68 ± 0.88	4.33 ± 0.75	12.59 ± 0.34	4.14 ± 0.39	13.49 ± 0.11	199.3
15b	4.75 ± 0.45	12.86 ± 0.26	5.1 ± 0.57	13.55 ± 0.70	4.75 ± 0.15	14.15 ± 0.24	177
15c	4.28 ± 0.21	17.40 ± 0.81	4.59 ± 0.74	12.83 ± 0.20	4.06 ± 0.40	13.95 ± 0.581	170.8
15d	4.21 ± 0.68	12.76 ± 0.34	4.94 ± 0.70	12.62 ± 0.57	4.56 ± 0.18	13.34 ± 0.37	259.1
15e	4.22 ± 0.20	5.58 ± 0.60	4.93 ± 0.83	14.04 ± 0.95	4.14 ± 0.58	14.94 ± 0.44	137.8
15f	4.41 ± 0.37	12.71 ± 0.14	4.41 ± 0.55	13.09 ± 0.93	4.46 ± 0.12	13.57 ± 0.86	329.2
15g	4.24 ± 0.25	12.05 ± 0.33	4.13 ± 0.80	13.28 ± 0.58	4.19 ± 0.11	14.29 ± 0.90	313.9
15h	4.13 ± 0.79	13.62 ± 0.28	4.43 ± 0.11	13.18 ± 0.12	4.06 ± 0.64	13.6 ± 0.82	264.8
15i	4.50 ± 0.28	12.97 ± 0.80	5.05 ± 0.76	13.99 ± 0.37	4.81 ± 0.89	15.06 ± 0.59	154.2
15j	4.65 ± 0.42	18.25 ± 0.51	4.81 ± 0.57	19.14 ± 0.86	4.14 ± 0.85	20.99 ± 0.93	13.49
15k	4.48 ± 0.76	11.98 ± 0.80	4.45 ± 0.25	14.43 ± 0.26	4.65 ± 0.68	15.7 ± 0.94	149.5
15l	4.66 ± 0.66	14.31 ± 0.21	4.71 ± 0.81	20.25 ± 0.16	4.61 ± 0.48	24.53 ± 0.43	11.7
Saline	4.98 ± 0.63	5.66 ± 0.94	4.86 ± 0.76	5.35 ± 0.14	4.61 ± 0.49	5.48 ± 0.19	3118
Morphine ¹	3.38 ± 0.26	10.6 ± 0.281	-	-	-	-	-

Racecadotril 4.21 ± 0.38 11.49 ± 0.33 4.57 ± 0.89 10.31 ± 0.81 4.25 ± 0.49 12.37 ± 0.66 **120.9**

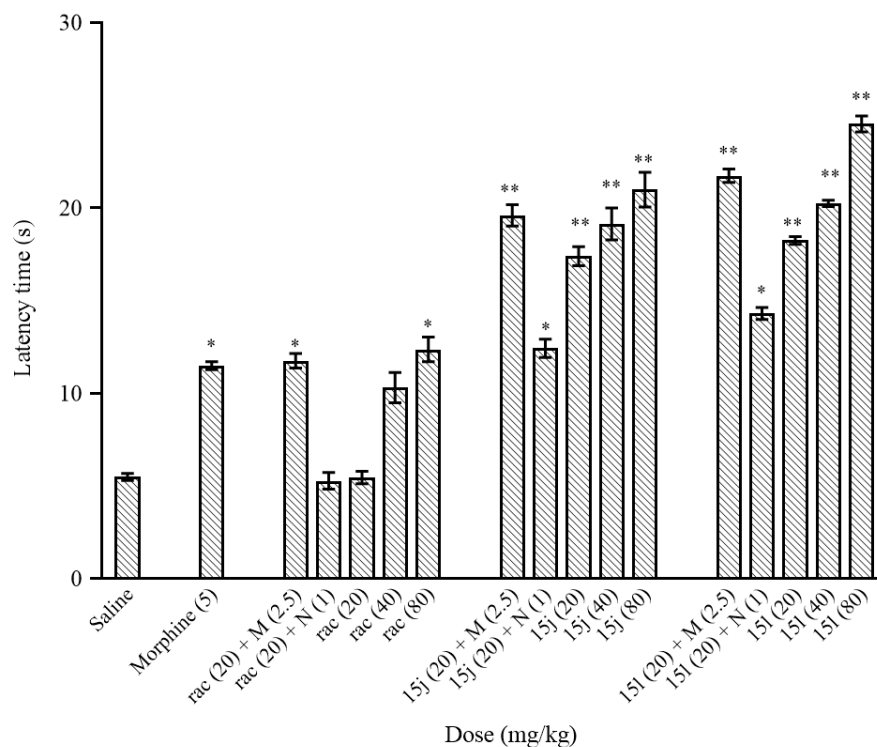


Fig. 2. Evaluation of synergic effects of racemic racecadotril and compounds **15j** and **15i** with morphine and antagonist effect of naloxone on racecadotril and compounds **15j** and **15i** in the hot plate test. The values represent mean ± SEM, n = 6. **P* < 0.05 and ***P* < 0.01 indicate significant differences from saline as the vehicle. M, Morphine; rac, racecadotril.

Table 2. Antinociceptive activity of the synthesized compounds 15a-l in comparison to morphine and racecadotril using the tail-flick test.

Compound	Latency time (s)						ED ₅₀ (mg/kg)
	20 mg/kg		40 mg/kg		80 mg/kg		
	0 min	60 min	0 min	60 min	0 min	60 min	
15a	3.37 ± 0.88	5.7 ± 0.69	3.49 ± 0.22	6.11 ± 0.44	3.48 ± 0.18	6.11 ± 0.40	595.8
15b	3.27 ± 0.18	5.26 ± 0.58	3.38 ± 0.59	7.85 ± 0.48	3.36 ± 0.80	7.85 ± 0.76	110.1
15c	3.3 ± 0.33	5.33 ± 0.56	3.47 ± 0.76	5.86 ± 0.55	3.42 ± 0.11	5.86 ± 0.38	516.7
15d	3.33 ± 0.17	4.73 ± 0.38	3.4 ± 0.71	5.94 ± 0.91	3.46 ± 0.56	5.94 ± 0.29	248.3
15e	3.39 ± 0.86	6.15 ± 0.77	3.42 ± 0.43	8.54 ± 0.54	3.24 ± 0.70	8.54 ± 0.82	91.32
15f	3.49 ± 0.37	6.4 ± 0.57	3.36 ± 0.77	7.88 ± 0.74	3.27 ± 0.53	7.88 ± 0.53	127.7
15g	3.24 ± 0.55	7.62 ± 0.46	3.42 ± 0.61	8.99 ± 0.48	3.34 ± 0.43	8.99 ± 0.56	79.86
15h	3.25 ± 0.89	7.69 ± 0.37	3.27 ± 0.51	9.64 ± 0.31	3.33 ± 0.11	9.64 ± 0.12	51.76
15i	3.43 ± 0.44	5.53 ± 0.49	3.49 ± 0.28	6.65 ± 0.07	3.5 ± 0.14	6.65 ± 0.48	234.4
15j	3.44 ± 0.54	9.61 ± 0.75	3.51 ± 0.74	12.9 ± 0.17	3.31 ± 0.11	14.6 ± 0.91	6.147
15k	3.27 ± 0.66	7.99 ± 0.59	3.44 ± 0.66	10.18 ± 0.13	3.29 ± 0.27	10.18 ± 0.95	38
15l	3.41 ± 0.67	9.12 ± 0.74	3.52 ± 0.12	12.65 ± 0.81	3.51 ± 0.31	14.11 ± 0.12	10.82
Saline	3.41 ± 0.46	3.45 ± 0.49	3.28 ± 0.10	3.62 ± 0.39	3.39 ± 0.17	3.4 ± 0.11	896.2
Morphine ¹	3.38 ± 0.26	10.6 ± 0.281	-	-	-	-	-
Racecadotril	3.25 ± 0.16	5.66 ± 0.12	3.24 ± 0.52	9.88 ± 0.64	3.39 ± 0.47	10.37 ± 0.78	53.69

¹Morphine was given at the dose of 5 mg/kg.

Table 3. The effect of the synthesized compounds 15a-l, morphine, and racecadotril on the number of licking after the injection of formalin into paw in mice.

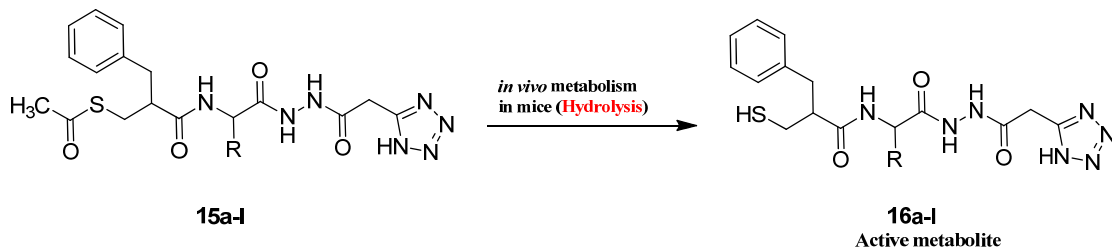
Compound	Concentration (mg/kg)	First phase Licking (min)	Second phase Licking (min)
15a	20	7.27 ± 0.47	8.85 ± 1.00
	40	7.12 ± 0.72	7.83 ± 0.36
	80	5.15 ± 0.29	4.08 ± 0.56
15b	20	7.27 ± 0.38	8.97 ± 0.88
	40	6.54 ± 0.34	8.52 ± 0.85
	80	5.15 ± 0.92	7.84 ± 1.03
15c	20	4.15 ± 0.54	7.03 ± 0.82
	40	7.01 ± 0.52	6.15 ± 1.00
	80	6.09 ± 0.63	4.58 ± 0.98
15d	20	7.27 ± 0.14	7.11 ± 0.95
	40	6.84 ± 0.57	6.98 ± 1.04
	80	6.29 ± 0.76	6.49 ± 0.44
15e	20	6.39 ± 0.84	8.44 ± 1.00
	40	7.13 ± 0.82	7.89 ± 0.82
	80	6.72 ± 0.30	7.03 ± 0.24
15f	20	6.88 ± 0.21	7.39 ± 0.22
	40	7.49 ± 0.57	6.98 ± 0.72
	80	7.33 ± 0.76	6.11 ± 0.31
15g	20	5.28 ± 0.59	6.35 ± 1.05
	40	6.23 ± 0.34	5.15 ± 0.35
	80	5.68 ± 0.11	4.78 ± 0.63
15h	20	6.88 ± 0.46	7.19 ± 0.21
	40	6.14 ± 0.44	6.72 ± 0.89
	80	5.28 ± 0.59	6.35 ± 1.05
15i	20	5.92 ± 0.31	8.68 ± 0.09
	40	7.27 ± 0.25	8.17 ± 0.61
	80	6.87 ± 0.29	7.74 ± 0.11
15j	20	4.21 ± 0.25	8.02 ± 0.26
	40	3.71 ± 0.40	6.19 ± 1.00
	80	3.11 ± 0.15	3.77 ± 0.26
15k	20	6.84 ± 0.63	7.11 ± 0.27
	40	6.29 ± 0.31	6.98 ± 0.19
	80	5.92 ± 0.22	6.49 ± 0.60
15l	20	5.09 ± 0.32	6.78 ± 0.16
	40	3.68 ± 0.50	5.89 ± 0.22
	80	2.24 ± 0.13	3.48 ± 0.11
Saline	90	7.32 ± 0.13	9.16 ± 0.89
Morphine	5	3.34 ± 0.08	2.86 ± 0.27
	20	6.09 ± 0.87	7.57 ± 0.34
Racecadotril	40	6.78 ± 0.65	7.15 ± 0.31
	80	6.34 ± 0.66	5.71 ± 0.36

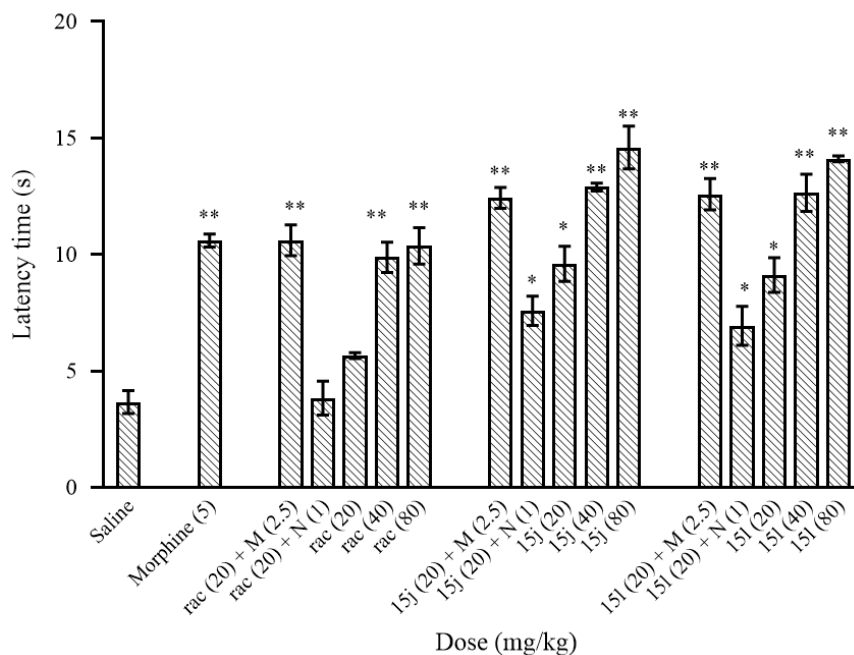
Docking study

The docking binding energies results are listed in Table 4. It is well documented in the literature that racecadotril rapidly hydrolyzed in plasma to its active metabolite, thiorphan, after oral administration (13,37). As the target compounds may undergo a similar hydrolytic reaction, nevertheless, we docked both unhydrolyzed forms of compounds **15a-l** (thioester) and hydrolyzed forms of compounds **16a-l** (thiol form, Scheme 2) in the catalytic site of NEP to examine the difference between their binding energies and interactions.

As shown in Table 4, all hydrolyzed forms showed better binding energies than their parent thioester forms. It seems that the hydrolyzed forms have a better ability to interact with NEP in comparison to its parent forms. However, the racecadotril and its metabolite thiorphan are exceptions. The tryptophan derivative **15l** and phenylalanine derivative **15j** exhibited the lowest values of binding energies than other compounds which are in good agreement with the experimental results.

The 3D and 2D interaction modes of the parent and hydrolyzed forms of the most active compounds **15j** and **15l** were shown in Fig. 4. The superimposed position clearly shows that all substituents placed well in the active site, and stay close to the Zn ion. The complete form of **15j** formed seven hydrogen bonds with the residues Arg 102, Asn 542, Ala 543, Tyr 545, His 583, Glu 584, and His 711. Interestingly, the coordination of the Zn atom with the residue of the side chain was extinguished and makes new ligation with three carbon atoms of the complete form of **15j** (Fig. 4A and E). The complete form of **15l**, interact with the active site with four hydrogen bonds with residues Asn 542, His 583, His 711, and Glu 646, and also the Zn coordination was observed (Fig. 4B and F). Both complete forms indicate a lot of hydrophobic interactions.



Scheme 2. Possible hydrolytic metabolism of compounds **15a-l** to active metabolites 16a-l.**Fig. 3.** Evaluation of synergic effects of racecadotril and compounds **15j** and **15i** with morphine and antagonist effect of naloxone on racecadotril and compounds **15j** and **15i** in the tail-flick test. The values represent mean \pm SEM, n = 6. * $P < 0.05$ and ** $P < 0.01$ indicate significant differences from saline as vehicle. M, Morphine; N, naloxone; rac, racecadotril.**Table 4.** Binding energies of synthesized compounds **15a-l** and racecadotril and hydrolyzed forms of them in the catalytic site of neprilysin.

Compound	Binding energy (kcal/mol)	Binding energy (kcal/mol) of the hydrolyzed form
15a	-8.24	-9.45
15b	-8.19	-8.94
15c	-7.39	-8.93
15d	-7.74	-9.73
15e	-6.75	-9.05
15f	-7.96	-9.98
15g	-7.19	-8.50
15h	-7.39	-8.36
15i	-6.61	-7.28
15j	-8.45	-12.21
15k	-7.40	-9.57
15l	-8.72	-12.32
Racecadotril	-8.88	-6.01

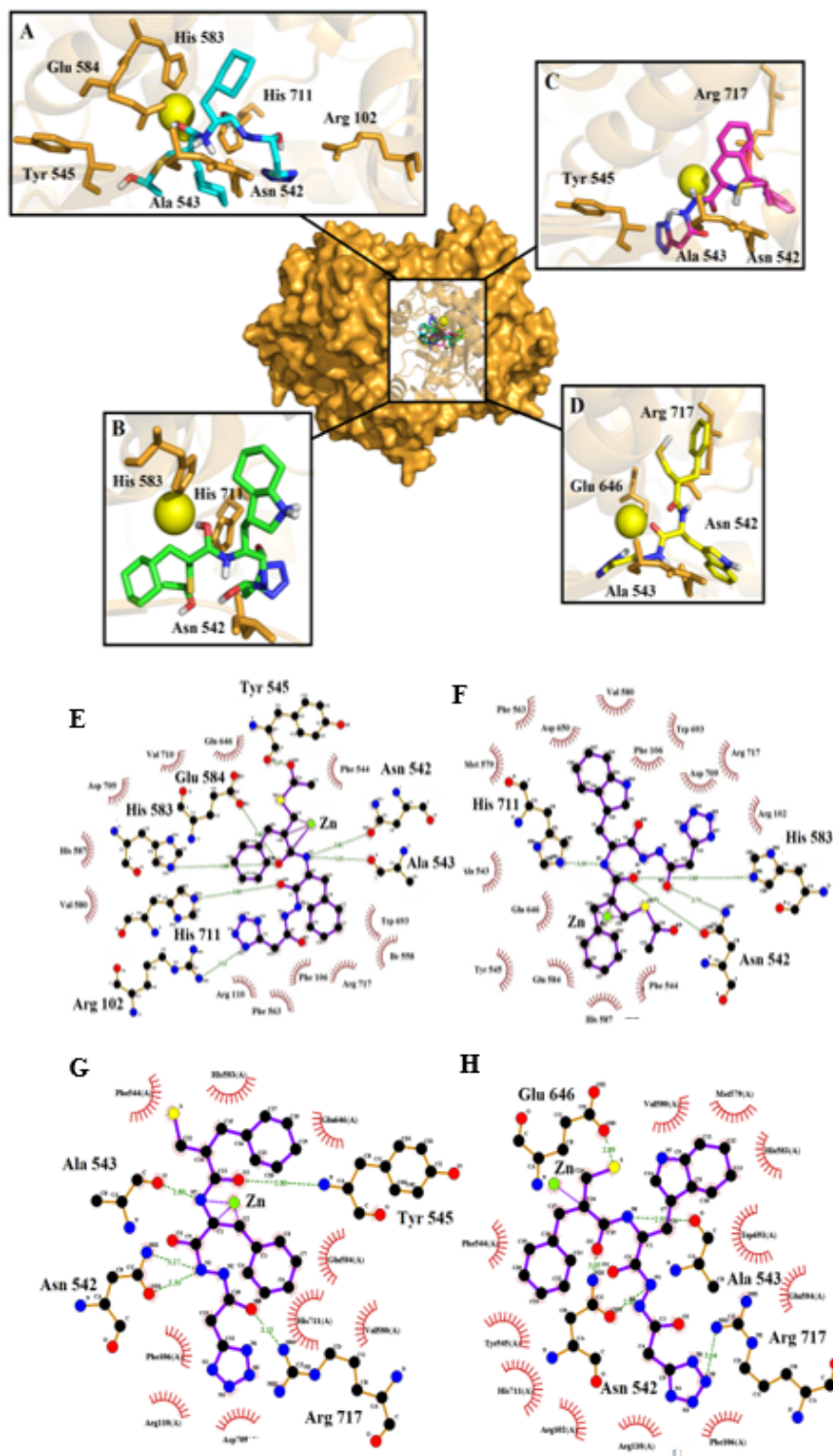


Fig. 4. Superimposed position of the most analgesic compounds in the catalytic site of NEP. The close interaction mode with residues and Zn ion in 3D and 2D displayed of the parent form of **15j** (**A**, **E**), **15i** (**B**, **F**), also hydrolyzed form of **15j** (**C**, **G**), and **15i** (**D**, **H**).

The hydrolyzed forms of compound **15j** established four hydrogen bonds with the residues Asn 542, Ala 543, Tyr 545, and Arg 717. This compound also coordinated with Zn ion as shown in Fig. 4C and G. The hydrolyzed forms of compound **15l** as another potent analgesic compound formed hydrogen bonds with Asn 542, Ala 543, Glu 646, and Arg 717 and coordinated with Zn ion (Fig. 4D and H). Both compounds **15j** and **15l** formed several hydrophobic interactions with NEP catalytic site.

It is interesting to note that in both thioester and hydrolyzed forms of a tryptophan derivative **15l** indicates a higher value of binding energy than the phenylalanine derivative **15j**. The cause can be found in hydrophobic interactions and the deep lipophilic cavity of the S'1 sub-site. The lipophilicity of substituted indole in tryptophan derivative is higher than phenyl ring in phenylalanine derivative, and also the space that they occupy is much larger and they fit well in the deep lipophilic cavity. Therefore, the superiority of tryptophan derivative in experimental assay and docking binding energy is due to the presence of the indole ring and its ability to interact properly with the active site.

DISCUSSION

As shown in scheme 1, the title compounds **15a-l** were synthesized in eight-step reactions. The structures of compounds **15a-l** were deduced based on IR, ^1H and ^{13}C NMR spectroscopy, MS, and elemental analysis. Representatively, the IR spectrum of **15j** showed absorptions at 3416 and 3479 (NH), 1726 (strong, C=O), and 1627 (strong, C=N) cm^{-1} . The mass spectrum of **15j** displayed the molecular ion (M^+) peak at $m/z = 509$. The ^1H NMR spectrum of **15j** exhibited two singlet signals recognized as arising from amines of the acetohydrazide and methyl of the thioacetyl groups ($\sigma = 10.10$ and 1.93 ppm, respectively). At the range of 3.17-2.52 ppm, the multiple peaks are due to the four methylene ($-\text{CH}_2-$) groups.

The CH group of the chiral center as multiple peaks and the CH group related to α carbon of amino acid were appeared in the range of

2.93-2.86 and 3.50 ppm, respectively. Characteristic signals with appropriate chemical shifts and coupling constants for the 8 protons of the aromatic moieties were observed in the aromatic region of the spectrum, and the amine of the amide functional group appears as a double with a coupling constant of 7.9 Hz, at 8.14 ppm. The ^1H decoupled ^{13}C NMR spectrum of **15j** showed six distinct aliphatic and eight distinct aromatic resonances, in agreement with the proposed structure. Three carbonyl groups and one thiocarbonyl group appeared in 164.0, 166.1, 171.9, and 184.6 ppm.

The result of the hot plate test revealed that the latency time values of the newly synthesized compounds **15a-l** demonstrated that all these compounds in all three used concentrations, except isoleucine derivative **15e** at 20 mg/kg, were more analgesic than racecadotril. It is worth noting that at 40 and 80 mg/kg, all new compounds acted better than morphine (5 mg/kg). The observed latency time values at 20 mg/kg of racecadotril-tetrazole-amino acid derivatives **15a-l** revealed that the better result was obtained with phenylalanine, valine, and tryptophan residues (compounds **15j**, **15c**, and **15l**, respectively). Tryptophan derivative **15l** and phenylalanine derivative **15j** at 40 and 80 mg/kg were more analgesics than other synthesized compounds. Moreover, the observed ED_{50} values also demonstrated that the most active compounds among the synthesized compounds in the hot-plate assay were compounds **15l** and **15j** with ED_{50} values of 11.7 and 13.49 mg/kg, respectively.

Tail flick assay's obtained-latency time values for the newly synthesized compounds demonstrated that these compounds at 20 mg/kg (range of latency times at 60 min = 4.73 ± 0.384 - 9.61 ± 0.756 s) have antinociceptive activity less than morphine at 5 mg/kg. On the other hand, among the new compounds **15a-l**, **15j** and **15l** at 40 and 80 mg/kg were more potent than morphine at 5 mg/kg. The comparison of latency times of the parent compound racecadotril with the new

compounds **15a-l** at 20 mg/kg revealed that compounds **15a**, **15e-h**, and **15j-l** were more potent than racecadotril. This comparison of 40 mg/kg exhibited that compounds **15j-l** acted better than racecadotril while at 40 mg/kg, only compounds **15j** and **15l** acted better than racecadotril. ED₅₀ values of the new compounds **15a-l** revealed that the most active compounds were compounds **15j** and **15l** with ED₅₀ values of 6.147 and 10.82 mg/kg, respectively.

Based on the formalin test results, most of the synthesized compounds and racecadotril at 20, 40, and 80 mg/kg did not show a plausible activity in the first and second phases of the formalin test in comparison to morphine at 5 mg/kg. Although compounds **15j** and **15l**, acted approximately similar to morphine in dose 5 mg/kg in two high doses 40 and 80 mg/kg in the first phase and high dose 80 mg/kg in the second phase.

The comparison of latency times of racecadotril-tetrazole-amino acid derivatives **15a-l** with 5-(1-(3-fluorophenyl)-1H-pyrazol-4-yl)-2H-tetrazole and 6-(4-chlorophenoxy)tetrazolo[5,1-a]phthalazine in hot plat test demonstrated that compounds **15a-l** had higher antinociceptive activity than previously reported tetrazoles when compared with morphine (19,20). On the other hand, the antinociceptive activity of D-phenylalanine was lower than phenylalanine derivative **15j** (38).

A docking study was performed to identify the possible interactions between synthesized compounds and the catalytic site of NEP as an enkephalinase. The main component of the catalytic site of this enzyme contains a central cavity with Zn ion and side chains residues of His 583, His 587, and Glu 646, which are coordinated with this atom, and also the deep lipophilic cavity of the S'1 subsite which is surrounded by residues Phe 106, Ile 558, Phe 563, Met 579, Val 580, Val 692, and Trp 693 (29). Re-docking of the co-crystal structure of ligand was used to validate the parameters and confirmation of the docking method. As shown in Fig. 5, the re-docked structure was well superimposed with a co-crystal ligand with RMSD lower than 2.

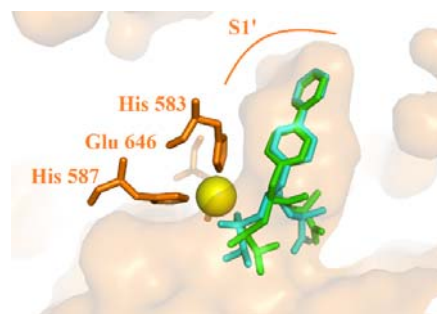


Fig. 5. Superimpose of co-crystal ligand (cyan) and re-docked ligand (green). The position of S'1 subsite of neprilysin and residue His 583, His 587, and Glu 646 which are coordinated with the zinc ion.

CONCLUSION

We have synthesized a series of novel racecadotril-tetrazole-amino acid derivatives **15a-l**, as potential antinociceptive agents. Our results demonstrated that racecadotril-tetrazole-amino acid derivatives **15a-l** have good to moderate antinociceptive activities in the performed assays, and among them, tryptophan derivative **15l** and phenylalanine derivative **15j** exhibited the highest analgesic effects. Antinociceptive activities of the latter compounds were comparable with morphine and higher than racecadotril. Compounds **15l** and **15j** also showed synergic effects with morphine and antinociceptive activities of these compounds were antagonized with naloxone. Docking study of these compounds in the catalytic site of NEP as an enkephalinase inhibitor was also in good agreement with the experimental section. These compounds could be used as a morphine replacement therapy without central side effects.

Acknowledgments

This work was financially supported by the Research Council of Tehran University of Medical Sciences, Tehran, I.R. Iran (Grant No. 96-01-33-34488).

Conflict of interest statement

The authors declared no conflict of interest in this study.

Author's contribution

All authors contributed equally to this work.

REFERENCES

- Bovill JG. Mechanisms of actions of opioids and non-steroidal anti-inflammatory drugs. *Eur J Anaesthesiol Suppl.* 1997;15:9-15.
DOI: 10.1097/00003643-199705001-00003.
- Holdgate A, Pollock T. Systematic review of the relative efficacy of non-steroidal anti-inflammatory drugs and opioids in the treatment of acute renal colic. *BMJ.* 2004;328(7453):1401.
DOI: 10.1136/bmj.38119.581991.55.
- Liles JH, Flecknell PA. The use of non-steroidal anti-inflammatory drugs for the relief of pain in laboratory rodents and rabbits. *Lab Anim.* 1992;26(4):241-255.
DOI: 10.1258/002367792780745706.
- Bagheri SM, Dashti RM, Morshedi A. Antinociceptive effect of *Ferula assafoetida* oleo-gum-resin in mice. *Res Pharm Sci.* 2014;9(3):207-212.
- Sethi N, Bhatti R, Ishar MPS. *In vivo* pharmacological profile of substituted (3-pyridyl)-2-phenylisoxazolidine analogues of nicotine as novel antinociceptives. *Res Pharm Sci.* 2014;9(1):59-67.
- Benyamin R, Trescot AM, Datta S, Ricardo Buenaventura M, Rajive Adlaka M, Nalini Sehgal M, et al. Opioid complications and side effects. *Pain Physician.* 2008;11(2 Suppl):S105-S120.
- Shah S, Mehta V. Controversies and advances in non-steroidal anti-inflammatory drug (NSAID) analgesia in chronic pain management. *Postgrad Med J.* 2012;88(1036):73-78.
DOI: 10.1136/postgradmedj-2011-130291.
- Szymaszkiewicz A, Storr M, Fichna J, Zielinska M. Enkephalinase inhibitors, potential therapeutics for the future treatment of diarrhea predominant functional gastrointestinal disorders. *Neurogastroenterol Motil.* 2019;31(4):e13526.
DOI: 10.1111/nmo.13526.
- Noble F, Roques BP. Protection of endogenous enkephalin catabolism as natural approach to novel analgesic and antidepressant drugs. *Expert Opin Ther Targets.* 2007;11(2):145-159.
DOI: 10.1517/14728222.11.2.145.
- Roques BP, Fournie-Zaluski MC, Wurm M. Inhibiting the breakdown of endogenous opioids and cannabinoids to alleviate pain. *Nat Rev Drug Discov.* 2012;11(4):292-310.
DOI: 10.1038/nrd3673.
- Hajhashemi V, Dehdashti K. Antinociceptive effect of clavulanic acid and its preventive activity against development of morphine tolerance and dependence in animal models. *Res Pharm Sci.* 2014;9(5):315-321.
- Salazar-Lindo E, Santisteban-Ponce J, Chea-Woo E, Gutierrez M. Racecadotril in the treatment of acute watery diarrhea in children. *N Engl J Med.* 2000;343(7):463-467.
DOI: 10.1056/NEJM200008173430703.
- Eberlin M, Muck T, Michel MC. A comprehensive review of the pharmacodynamics, pharmacokinetics, and clinical effects of the neutral endopeptidase inhibitor racecadotril. *Front Pharmacol.* 2012;3:93-108.
DOI: 10.3389/fphar.2012.00093.
- Roques BP, Fournie-Zaluski MC, Soroca E, Lecomte JM, Malfroy B, Llorens C, et al. The enkephalinase inhibitor thiorphan shows antinociceptive activity in mice. *Nature.* 1980;288(5788):286-288.
DOI: 10.1038/288286a0.
- Yamamori Y, Saito Y, Kaneko M, Kirihara Y, Sakura S, Kosaka Y. Antinociceptive effects of ONO-9902, an enkephalinase inhibitor, after visceral stress condition in rats. *Can J Anaesth.* 1996;43(11):1175-1179.
DOI: 10.1007/BF03011848.
- Fournie-Zaluski MC, Chaillet P, Bouboutou R, Coulaud A, Cherot P, Waksman G, et al. Analgesic effects of kelatorphan, a new highly potent inhibitor of multiple enkephalin degrading enzymes. *Eur J Pharmacol.* 1984;102(3-4):525-528.
DOI: 10.1016/0014-2999(84)90575-2.
- Lambert DM, Mergen F, Poupaert JH, Dumont P. Analgesic potency of *S*-acetylthiorphan after intravenous administration to mice. *Eur J Pharmacol.* 1993;243(2):129-134.
DOI: 10.1016/0014-2999(93)90371-n.
- Ballatore C, Huryn DM, Smith 3rd AB. Carboxylic acid (bio)isosteres in drug design. *ChemMedChem.* 2013;8(3):385-395.
DOI: 10.1002/cmdc.201200585.
- Florentino IF, Galdino PM, De Oliveira LP, Silva DP, Pazini F, Vanderlinde FA, et al. Involvement of the NO/cGMP/KATP pathway in the antinociceptive effect of the new pyrazole 5-(1-(3-fluorophenyl)-1*H*-pyrazol-4-yl)-2*H*-tetrazole (LQFM-021). *Nitric Oxide.* 2015;47:17-24.
DOI: 10.1016/j.niox.2015.02.146.
- Yu HL, Zhang F, Li YJ, Gong GH, Quan ZS. Anti-inflammatory and antinociceptive effects of 6-(4-chlorophenoxy)-tetrazolo[5,1-*a*]phthalazine in mice. *Pharmacol Rep.* 2012;64(5):1155-1165.
DOI: 10.1016/s1734-1140(12)70912-x.
- Asadi P, Khodarahmi G, Jahanian-Najafabadi A, Saghaie L, Hassanzadeh F. Biologically active heterocyclic hybrids based on quinazolinone, benzofuran and imidazolium moieties: synthesis, characterization, cytotoxic and antibacterial evaluation. *Chem Biodivers.* 2017;14(4):e1600411.
DOI: 10.1002/cbdv.201600411.
- Nalivaeva NN, Zhuravin IA, Turner AJ. Neprilysin expression and functions in development, aging and disease. *Mech Ageing Dev.* 2020;192:111363.
DOI: 10.1016/j.mad.2020.111363.
- Ramirez-Sanchez M, Prieto I, Segarra AB, Martinez-Canamero M, Banegas I, de Gasparo M. Enkephalinase regulation. *Vitam Horm.* 2019;111:105-129.
DOI: 10.1016/bs.vh.2019.05.007.
- Lu D, Vince R. Discovery of potent HIV-1 protease inhibitors incorporating sulfoximine functionality. *Bioorg Med Chem Lett.* 2007;17(20):5614-5619.
DOI: 10.1016/j.bmcl.2007.07.095.

25. Rürger N, Roatsch M, Emmrich T, Franz H, Schüle R, Jung M, *et al.* Tetrazolylhydrazides as selective fragment-like inhibitors of the JumonjiC-domain-containing histone demethylase KDM4A. *ChemMedChem*. 2015;10(11):1875-1883. DOI: 10.1002/cmdc.201500335.
26. Senokuchi K, Nakai H, Nagao Y, Sakai Y, Katsube N, Kawamura M. New orally active enkephalinase inhibitors: their synthesis, biological activity, and analgesic properties. *Bioorg Med Chem*. 1998;6(4):441-463. DOI: 10.1016/S0968-0896(97)10048-7.
27. Bloom AS, Dewey WL, Harris LS, Brosius KK. The correlation between antinociceptive activity of narcotics and their antagonists as measured in the mouse tail-flick test and increased synthesis of brain catecholamines. *J Pharmacol Exp Ther*. 1976;198(1):33-41.
28. Hunskaar S, Fasmer OB, Hole K. Formalin test in mice, a useful technique for evaluating mild analgesics. *J Neurosci Methods*. 1985;14(1):69-76. DOI: 10.1016/0165-0270(85)90116-5.
29. Oefner C, Roques BP, Fournie-Zaluski MC, Dale GE. Structural analysis of neprilysin with various specific and potent inhibitors. *Acta Crystallogr D Biol Crystallogr*. 2004;60(Pt 2):392-396. DOI: 10.1107/S0907444903027410.
30. Morris GM, Huey R, Lindstrom W, Sanner MF, Belew RK, Goodsell DS, *et al.* AutoDock4 and AutoDockTools4: automated docking with selective receptor flexibility. *J Comput Chem*. 2009;30(16):2785-2791. DOI: 10.1002/jcc.21256.
31. Hosseini FS, Amanlou M. Anti-HCV and anti-malaria agent, potential candidates to repurpose for coronavirus infection: virtual screening, molecular docking, and molecular dynamics simulation study. *Life Sci*. 2020;258:118205. DOI: 10.1016/j.lfs.2020.118205.
32. Khodarahmi G, Asadi P, Farrokhpour H, Hassanzadeh F, Dinari M. Design of novel potential aromatase inhibitors *via* hybrid pharmacophore approach: docking improvement using the QM/MM method. *RSC Adv*. 2015;5(71):58055-58064. DOI: 10.1039/C5RA10097F.
33. Santos-Martins D, Forli S, Ramos MJ, Olson AJ. AutoDock4_{zn}: an improved AutoDock force field for small-molecule docking to zinc metalloproteins. *J Chem Inf Model*. 2014;54(8):2371-2379. DOI: 10.1021/ci500209e.
34. Yuan S, Chan HS, Hu Z. Using PyMOL as a platform for computational drug design. *WIREs Comput Mol Sci*. 2017;7(2):e1298. DOI: 10.1002/wcms.1298.
35. Laskowski RA, Swindells MB. LigPlot+: multiple ligand-protein interaction diagrams for drug discovery. *J Chem Inf Model*. 2011;51(10):2778-2786. DOI: 10.1021/ci200227u.
36. Andujar-Sanchez M, Camara-Artigas A, Jara-Perez V. A calorimetric study of the binding of lisinopril, enalaprilat and captopril to angiotensin-converting enzyme. *Biophys Chem*. 2004;111(2):183-189. DOI: 10.1016/j.bpc.2004.05.011.
37. Xu Y, Huang J, Liu F, Gao S, Guo Q. Quantitative analysis of racecadotril metabolite in human plasma using a liquid chromatography/tandem mass spectrometry. *J Chromatogr B Analyt Technol Biomed Life Sci*. 2007;852(1-2):101-107. DOI: 10.1016/j.jchromb.2006.12.041.
38. Halpern LM, Dong WK. D-phenylalanine: a putative enkephalinase inhibitor studied in a primate acute pain model. *Pain*. 1986;24(2):223-237. DOI: 10.1016/0304-3959(86)90045-X.